International Forum on Aeroelasticity and Structural Dynamics
IFASD 2019
9-13 June 2019, Savannah, Georgia, USA

CPACS-MONA – AN INDEPENDENT AND IN HIGH-FIDELITY BASED MDO TASKS INTEGRATED PROCESS FOR THE STRUCTURAL AND AEROELASTIC DESIGN OF AIRCRAFT CONFIGURATIONS

T. Klimmek[1], M. Schulze[1], M. Abu-Zurayk[2], C. Ilic[2], and A. Merle[2]

[1]DLR, German Aerospace Center
Institute of Aeroelasticity
Bunsenstr. 10, 37073 Göttingen Germany
thomas.klimmek@dlr.de
matthias.schulze@dlr.de

[2]DLR, German Aerospace Center
Institute of Aerodynamics and Flow Technology
Lilienthalplatz 7, 38108 Braunschweig Germany
mohammed.abu-zurayk@dlr.de
caslav.ilic@dlr.de

Keywords: High-fidelity based MDO, loads analysis, aeroelastic design, parametric modelling, cpacs-MONA

Abstract: The highly parameterized aeroelastic structural design process cpacs-MONA for simultaneous structural and aeroelastic design of the load carrying structure of an aircraft configuration is presented. The process consists of preliminary mass and loads estimation based on conceptual design methods followed by a parameterized set-up of simulation models and an optimization model. These models are used for a comprehensive loads analysis followed by a component wise structural optimization. The latter takes stress, strain, buckling and control surface efficiency as constraints into account. The detailed structural modelling allows also for the use of well-established structural optimization methods. The data basis for the simulation models and the various analyses is a suitable CPACS dataset.

The design process cpacs-MONA is also part of various high-fidelity based MDO processes developed at DLR, where also other disciplines like for example aerodynamics and overall aircraft design are involved. In this paper three applications are presented for cpacs-MONA. In the first one cpacs-MONA is applied as an independent and stand-alone aeroelastic structural design process for the XRF1-DLR baseline configuration followed by the investigation of a number of geometrical variations regarding the wing aspect ratio and the wing sweep. Lastly the results for the structural design of cpacs-MONA are examined within the high-fidelity based MDO approach following the so-called cybermatrix protocol. Therein aerodynamic optimization, structural optimization, and loads analysis run independently in parallel with a coupling due to a regular exchange of defined parameters.

1 INTRODUCTION

Aeroelastic structural design has been becoming more and more important for the structural design of aircraft components. Furthermore, together with the aerodynamic design it is a central aspect of the overall design of an aircraft. This is especially the case for the concurrent consideration of aerodynamic and structural design in the field of multidisciplinary

optimization (MDO). For high-fidelity based MDO tasks in aircraft design, where the high-fidelity part is mainly covered by computational fluid dynamics (CFD) aerodynamic analysis or coupled aero-structural analysis and optimization, a proper incorporation of the aeroelastic structural design is indispensable.

Due to the term “aeroelastic structural design” the necessity to include the effects of the flexibility of the structure is expressed. This is also reflected by the fact that for large aircraft the flexibility of the structure cannot be neglected anymore regarding the loads, the performance, and the maneuverability of an aircraft. The roots of aeroelastic structural design are grounded in developed structural optimization methods, where structural and aeroelastic requirements are concurrently taken into account. Methods have been made applicable over several decades. Exemplarily the commercial computer programs MSC Nastran [1] and ASTROS [2], as well as MBB-Lagrange [3] can be named.

In the course of the time frameworks for aeroelastic structural design were developed where especially optimization methods dealing with composite fiber material were set-up [4]. Another development is the incorporation of aeroelastic structural design into the aircraft design processes in order to establish a coupling with aerodynamics to the point of high-fidelity-based multidisciplinary aero-structural optimization. For such high-fidelity-based MDO implementations on the one hand the classical path regarding mathematical optimization is pursued, where gradients of the objective and defined constraints with respect to the design variables are used [5]. On the other hand and especially stimulated by the todays availability of massive computational power, gradient-free approaches also with high-fidelity-based analysis methods seem to be promising [6]. A third alternative is the multi-level approach where aerodynamic optimization is done on the upper level and structural optimization and other disciplinary applicable sub-optimizations are done on a lower level [7], [8].

The structure of the paper is as follows. First, the basic aeroelastic structural design process MONA is described, where the aspect of the parameterization of all involved simulation and optimization models is the key. Then the advanced tool-like aeroelastic structural design process cpacs-MONA is depicted in detail. The application of cpacs-MONA to the XRF1-DLR configuration is shown with its results for the baseline configuration and further geometrical parameter variations regarding the wing. Finally, the results regarding the structural design for an application of the process in a gradient-free high-fidelity based MDO environment, the cybermatrix protocol, are discussed.

2 MONA - A BASIC PROCESS FOR AEROELASTIC STRUCTURAL DESIGN

Aeroelastic structural design comprises in particular the consideration of the loads of the flexible structure and aeroelastic requirements like sufficient control surfaces efficiency or the avoidance of flutter within the aeroelastic stability envelope. Furthermore carbon fiber reinforced plastic is offering an important aspect for aeroelastic structural design by an optimized utilization of material properties. The latter is well known as “aeroelastic tailoring”. Finally also flight control techniques applied for loads analysis or with regards to flutter can be included into the aeroelastic structural design process.

A basic aeroelastic structural design process can be defined by two steps: 1. Loads analysis with the flexible structure and 2. Structural design, using structural optimization methods, where also aeroelastic constraints are taken into account. Presupposed a reasonable first guess for the structural design (e.g. thickness of skins, spars and ribs) is available, such process can

be run through until convergence with respect to the structural weight and the loads is achieved. In order to insure consistency of the simulation and optimization models for the loads analysis and the structural optimization and to be able to deal with various aircraft configurations regarding various construction concepts, at the DLR Institute of Aeroelasticity (DLR-AE) a specific parameterization concept has been developed over the last almost 20 years.

The computer program ModGen was developed to insure the previously mentioned consistency of the models. It sets up all the necessary simulation and optimization models for the aeroelastic structural design process. With ModGen upstream the kernel aeroelastic structural design process at DLR-AE, named MONA is pursued. It consists of three steps as shown in Figure 1. The name MONA refers to the main computer programs that are used. It's at first the already mentioned computer program **Mo**dGen for the model set-up and MSC **Na**stran of the loads analysis and the structural optimization.

The parametric model set-up with ModGen is based on parametrically defined geometry models of the wing-like components and the fuselage This comprises the outer geometry and all significant elements of the load carrying structure. Thereby *B*-splines are used because of their smooth curve and surface characteristics. Differential geometrical design methods are part of the successive geometry model set-up process. The basic MONA process in far more detail is described in [9]. In Figure 1 the in principle available options of MONA are shown.

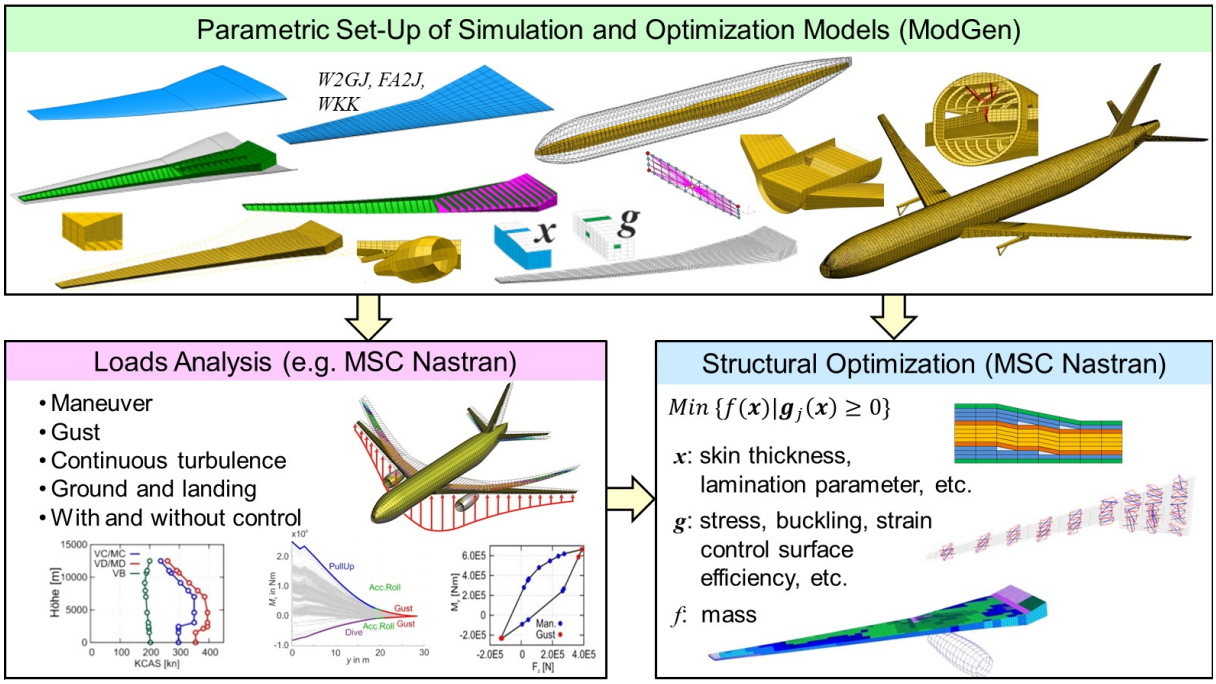

Figure 1: Basic MONA process.

An application of the MONA process is the set-up of a structural model to be used for aeroelastic investigations for the CRM configuration [10]. Another example of partly using MONA by only replacing the loads analysis part, the so-called LoadsKernel, is shown in [11]. An advanced usage of the in the later described process cpacs-MONA by additional structural optimization for composite material using lamination parameters as design variables for the purpose of setting-up a structural model for the XRF1-DLR configuration is outlined in [12]. Regarding the possible modelling capabilities, in [13], where ground loads are investigated, a

complete and component wise detailed structural finite element model (wing-like components and fuselage) for the DLR-D150 configuration was set up.

3 CPACS-MONA– STAND-ALONE PROCESS AND SUB-PROCESS IN MDO ENVIRONMENTS

The tool-like design process cpacs-MONA is based on MONA, but cpacs-MONA exhibits a far more automatization of the process, in order to be used as a tool in more extensive design and MDO environments [14]. Another outstanding feature of cpacs-MONA is the interfacing with a proper CPACS dataset of an aircraft configuration.

The Common Parametric Aircraft Configuration Schema (CPACS) is a data definition using XML text format for the air transportation system [15]. CPACS describes a wide range of characteristics of the aircraft, like the geometry, global aircraft parameter, the structural construction concept, material data etc., in a structured, hierarchical manner. Not only product but also process information is stored in CPACS, like aerodynamic data, aircraft loads, or mass data. CPACS is not limited to aircraft it also covers rotorcraft, engines, climate impact, fleets and mission data.

cpacs-MONA reads from the CPACS dataset information about the wing planform, the wing topology like ribs, spars and stringer positions and initial thicknesses together with the engine, pylon and landing gear positions and dimensions. It also uses information about aircraft masses like design, primary and secondary masses plus the dimensions of the control surfaces and fuel tanks. As optional input Tecplot profile cuts from the outer geometry of the aircrafts wings and the engine, generated from a CAD-model, can be used. The profile cuts will then be migrated into the existing CPACS dataset and the outer shape of the engine and its center of gravity will be updated.

In the following the process steps are described in more detail. Figure 2 shows the process flow of cpacs-MONA.

3.1 Conceptual design loads

An estimation of loads with methods from conceptual design has been developed and implemented to provide proper loads for the dimensioning of the initial structural model. The input parameters are the global aircraft parameters, like the design masses, typical parameters for the wing like aspect ratio, wing area, wing sweep, kink position, and engine position. The results are cutting loads and loads distributed over the so-called load reference axis (LRA) of the aircraft.

3.2 Conceptual design stiffness estimation

The estimated cutting loads are then used to compute the dimensions of the loads carrying structure. Simplified rectangle cross sections for the structural wing box and circular cross sections for the fuselage are subjected section-wise to the cutting loads. For the cross-sections of the wing stringer, spar-caps, and inner stiffener for the spars and ribs, and for the fuselage stringer and frames are taken into account as reinforcement structure. It is assumed that the wing skins carry wing bending moments, while the spars and ribs resist shear and torsional loads. Fuselage loads are accounted with and without cabin pressure differential according to the EASA regulations CS25.365(a) and CS25.365(d).

Together with further material data and the allowable stress values the dimensions for the skins, spars (both section wise), and ribs of the wing and the skin of the fuselage are estimated as well as the required areas for the stringers, the spar-caps, the inner rib and spar stiffeners, and the frames. As allowable stresses ultimate, yield and fatigue are included. Buckling is incorporated for the wing and the fuselage in a simplified and knowledge based manner.

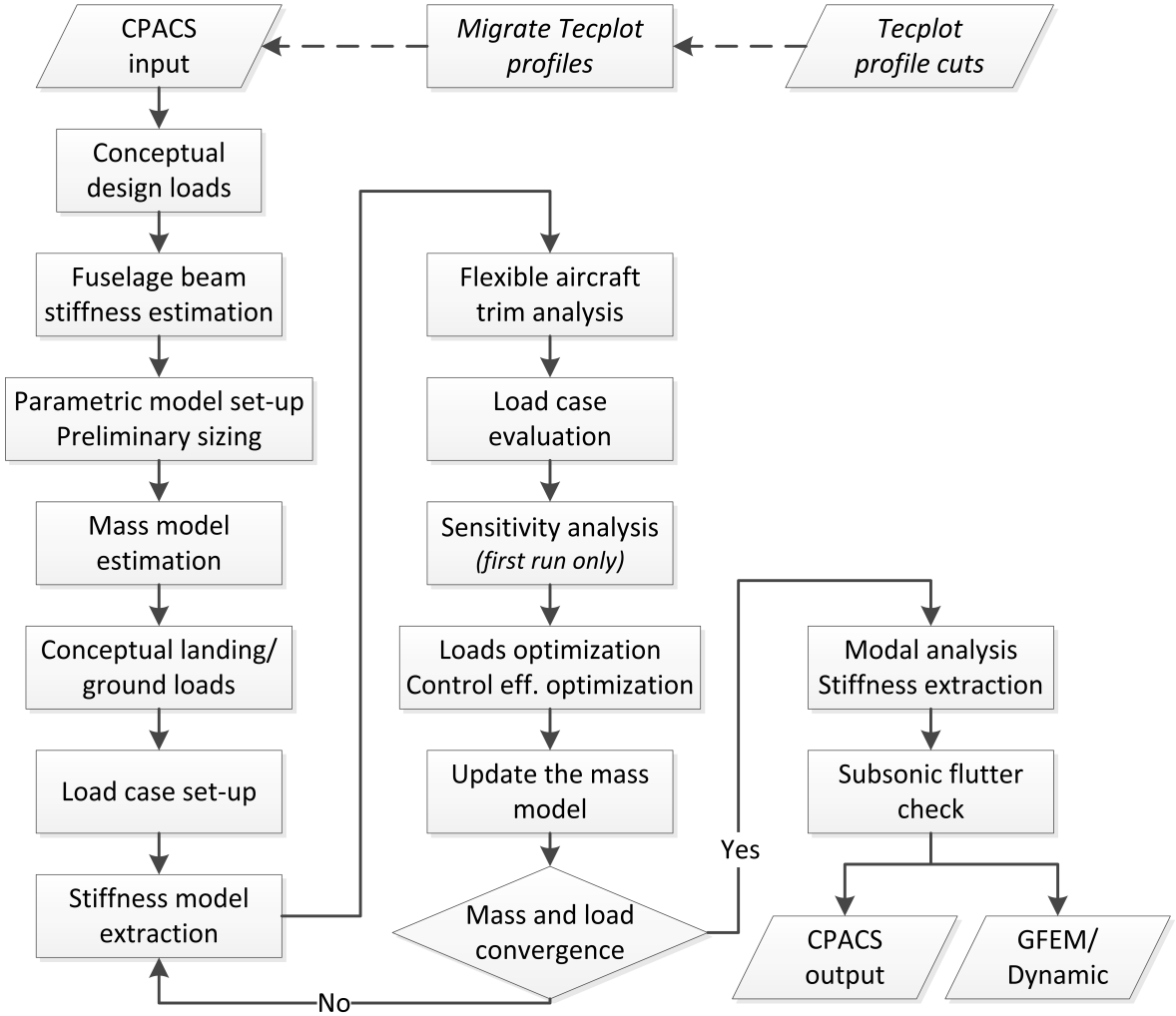

Figure 2: Process flow of cpacs-MONA.

3.3 Conceptual design mass model

For proper loads- and aeroelastic analysis a reasonable mass model has to be set-up. Therefore a mass model for the operation weight empty (OWE) configuration and mass models for defined payload, passenger, and fuel configurations are established. The OWE mass configuration can be split into the mass items representing the structure (primary, secondary and further non-structural masses as fittings) and the mass items for systems, equipment, and furniture. For the structural mass the estimated total mass values for each component are portioned into mass items per loads reference point.

In the same way the estimated total fuel mass and percentage quantities are distributed proportionally to their volume along the load reference axis of the wing. The boundaries of the fuel tanks are taken into account. For payload and passenger masses, distributed mass items for the fuselage are created according to the individually defined payload, passenger configurations. In cases a detailed fuselage mass model for furnishing, systems, and operator

items located in the fuselage, is available, e.g. created by the cabin design tool FUCD [16], the corresponding mass parameters are part of the CPACS dataset. Otherwise estimated total mass values and a corresponding center of gravity value are taken into account. Finally distributed masses are lumped into one mass item per LRA point.

3.4 Set-up of the load cases

The considered load cases comprise maneuver loads, gust loads via the approach according to Pratt, and ground loads. A flight envelope is set up according to CS25.335 requirements for the given or approximated design speeds V_C/M_C and V_D/M_D, where V_C is set to V_{MO}. V_{MO} is either given in the CPACS dataset or approximated on the given target cruise speed M_{cruise} at service ceiling level. The stall speed V_S and the maneuver speed V_A are estimated on provided values of $c_{l,\max}(Ma)$, $c_{l,\min}(Ma)$, and $c_{l,\alpha}(Ma)$. A load maneuver and gust load case is finally defined by a distinct flight point (speed and altitude) a vertical load factor and a specified mass configuration. Regarding the trim conditions for the maneuver and gust load calculation symmetric pull-up and push-down as well as yawing and rolling are considered.

3.5 Set-up of the simulation- and optimization models

The set-up of the structural models is done for the wing-like components with ModGen. The load carrying wing box structures for MSC Nastran are created according to the structural concept defined in the CPACS dataset. Starting from the outer geometry (profiles, segments) the spars are located and the ribs distributed between front and rear spar. For the resulting geometrical objects out of the intersection of spars, ribs and skin, iso-parametric meshes are created individually, where in addition to the shell elements for the skin, spars, and ribs, reinforcing structural elements (e.g. stringer, spar caps, inner stiffener for spars and ribs) are modelled with beam elements. Due to consistent partition parameters at the edges of the geometrical surfaces that are meshed, a continuous finite element model mesh is ensured. The pylon is modelled with beam elements. Their structural properties for the beams are based on empirical knowledge of comparable aircraft configurations regarding the structural dynamic characteristics of the pylon with attached engine. Using defined Multi Point Constraint elements (e.g. RBE2) the assembly to the point of a complete structural stiffness model for the aircraft configuration is achieved. Interpolation elements (e.g. RBE3 with UM option) are in addition defined to create a to the load reference axis condensed stiffness model.

The mass model for the structure and the corresponding payload, passenger, fuel configuration, in terms of concentrated mass elements, is basically taken from the mass model set up of the conceptual design mass estimation (see section 3.3).

The aerodynamic model set-up consists of the definition of lifting surfaces for the vortex and doublet lattice method (VLM and DLM) as macro panel elements for each component (wing, horizontal and vertical tail, and fuselage). They are merged to a complete and gap-free model due to coordinated definitions of their planform geometry. The control surfaces like elevator, rudder, and aileron are defined by the specifying the respective aerodynamic boxes and coordinate systems for the rotation axes. For the wing-like components the characteristics of the camber lines are taken into account (W2GJ matrices set up by ModGen) and for the fuselage a reasonable decrease of $c_{l,\text{a}}$ due to non-optimal lift characteristics based on [17] is included. For the coupling of the aerodynamic model to the structural model the grid points of the load reference axes are taken as well as grid points located at the intersection of the rib planes and the leading and trailing edge of the aerodynamic macro panels. These grid points are rigidly connected to a corresponding grid point of the load reference axis. The trim

conditions of for the trim analysis (e.g. n_z, roll rate, pitch velocity, gear velocity) for the individual load cases are taken from the load case set-up.

The optimization model is set-up for the wing-like components individually as the structural optimization to estimate the structural thickness properties is also done individually per wing-like component. The optimization model consists of the definition of the design variables, the constraints, and an objective. The design variables comprise the thickness of a design region. The design regions of the wing box are on the one hand the partial skin surfaces, surrounded by spars and ribs, and the partial rib and spar surfaces due to their intersections among each other. The dimensions of the stiffener elements (e.g. stringer, spar caps) are not part of the optimization model. Regarding the constraints allowable stress values per shell element are defined. They are based on yielding, ultimate strength, and local buckling. The latter considers simultaneous skin and stringer buckling modes according to [18]. The objective is the structural mass of the individual component to be minimized.

3.6 Load analysis

The loads are estimated mainly due to quasi static trim analysis using MSC Nastran SOL144. Per mass configuration the trim simulations for various trim conditions are executed. The results are forces and moments acting at the grid points of the load reference axes. These loads are called nodal loads. They contain the contribution from aerodynamic side and the inertia part.

In order to select the design loads for the structural optimization, the so-called cutting loads for the shear force, the bending, and the torsional moments (SMT-loads) are estimated and analyzed for selected monitor stations. All load cases forming the envelope of the cutting load components F_z/M_x and M_x/M_y are picked as design load cases. This is done for the wing, the horizontal tailplane, the vertical tailplane, and the fuselage individually. For chosen load cases the nodal loads are made available for the structural optimization.

3.7 Analytical empirical pre-sizing and structural optimization

The estimation of the structural dimensions of the wing-like components is done in three steps. In the first step the structural properties, such as skin, spar, rib thickness and the cross-section area of stringer, spar caps and inner stiffener are based on the provided cutting loads of the resulting conceptual design load cases as described in section 3.1. The used analytical and empirical pre-sizing method corresponds to the method described in section 3.2. This analytical empirical pre-sizing is also called preliminary cross section sizing (PCS). It is executed when the simulation models are set up. Adapted structural models for the wing-like components are available for the next step. After the extensive loads evaluation described in section 3.6, the PCS is performed a second time with the more reliable loads to get a better starting point for the 3rd iteration.

Within the 3rd iteration mathematical optimization algorithms are applied, using MSC Nastran SOL200 [1]. The proper dimensioning of the load carrying structure, where the established finite elements models come into play, is treated as structural optimization task. This task is solved with methods from mathematical optimization, also called mathematical programming. The optimization is formulated as follows:

$$Min\{f(\boldsymbol{x})|\boldsymbol{g}(\boldsymbol{x}) \leq 0;\ \boldsymbol{x}_l \leq \boldsymbol{x} \leq \boldsymbol{x}_u\} \tag{1}$$

with f as the objective function, $\boldsymbol{x}$ as the vector of n design variables, $\boldsymbol{g}$ as the vector of m_g inequality constraints. The definition of the objective function f, the design variables $\boldsymbol{x}$, and the constraints $\boldsymbol{g}$ is called optimization model. As objective function f, the mass of the wing box is defined. According to section 3.5 the design variables are thicknesses of the defined design fields. For a first structural optimization step various stress values are defined as constraints.

In a second structural optimization step the resulting thicknesses of the design fields from the first optimization step are defined as lower bound regarding the design variables, and the aileron efficiency is the only constraint. The objective is still the structural mass of the wing box.

This approach of two sequential structural optimization runs is used on the one hand to estimate the additional mass needed to comply with the control surface efficiency constraint. It also on the other hand eases the structural optimization step with stress constraints, because the mixture of various types of constraints for one optimization task can be challenging regarding the convergences of the optimization.

3.8 Update of the CPACS dataset and rerun of cpacs-MONA

After the structural optimization for each wing-like component converged according to the defined convergence criteria, the resulting structural mass of the wing box is written into the CPACS dataset. Then the loads analysis is done again using the structural properties from the previous structural optimization, the design loads are estimated, and the structural optimization is performed again. This process of loads analysis, design loads estimation, and structural optimization is repeated until the change of the structural mass and the maximum bending moment of all wing-like components (wing, horizontal tailplane, and vertical tailplane) of two sequential iterations is below 0.1%. Finally also a flutter analysis using MSC Nastran SOL145 is performed. This is done to check the subsonic flutter characteristics of the established structural model of the complete aircraft configuration.

4 REFERENCE AIRCAFT CONFIGURATION

As reference configuration for this paper the generic research aircraft called XRF1 is used. The XRF1 is a long range wide body transport aircraft developed by Airbus as part of the eXternal Research Forum (XRF). This research platform is used for collaborations between Airbus, research institutions and universities. Figure 3 shows the outer geometry of the XRF1.

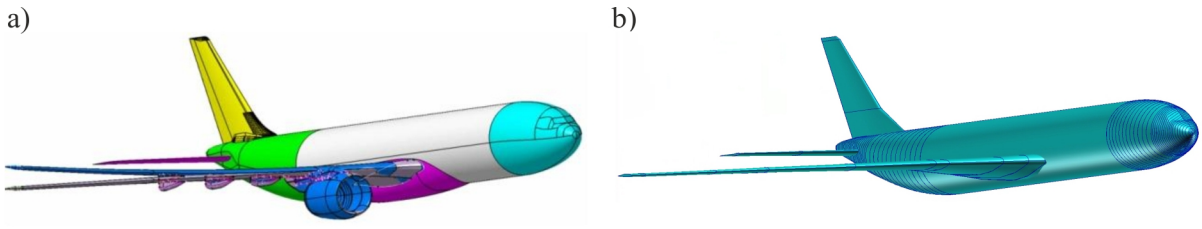

Figure 3: General view of Airbus XRF1 Research geometry (wing in jig and flight shape) [19] and XRF1-DLR IGES Geometry from CPACS dataset created with TIGL viewer [20].

The top-level aircraft requirements of the XRF1 are similar to the long range aircraft Airbus A330-300. A CPACS dataset describing the Airbus XRF1 was set up for the DLR project Digital-X [21] and is under further development within the DLR project VicToria [22]. cpacs-MONA uses this CPACS dataset for the model generation. The resulting configuration is

called XRF1-DLR. The characteristic attributes of the XRF1-DLR are shown in Table 1. The aircraft structure is modelled with aluminum. In [12], the generated XRF1-DLR from cpacs-MONA was further developed and the aluminum properties have been replaced with composite, leading to the so called XRF1-DLR-C.

Table 1: Characteristics of the XRF1-DLR configuration.

Span, m	Wing area, m^2	AR	LE sweep, deg.	Ref. chord, m	MTOW, kg	OWE, kg
57.99	374	8.99	32.0	6.45	245000	128000

As an output of the cpacs-MONA process the full structural finite element model for MSC Nastran is created. In Figure 4a) the right half of the model is displayed. It is also called GFEM/dynamic (GFEM ≙ global finite element model), which expresses the applicability of the structural model for dynamic analysis. Such characteristic is especially required for dynamic aeroelastic analysis like gust load or flutter analysis. As can be seen in Figure 4a), the stiffness of the fuselage is until now approximated with pre-sized beam elements. One ongoing development in ModGen is the full model generation of the fuselage with details like frames, pressure bulkheads, keel beam, wing integration, etc. (see also Figure 1) and will later be used within the cpacs-MONA process. The topology of the wing with its element types is shown in Figure 4b).

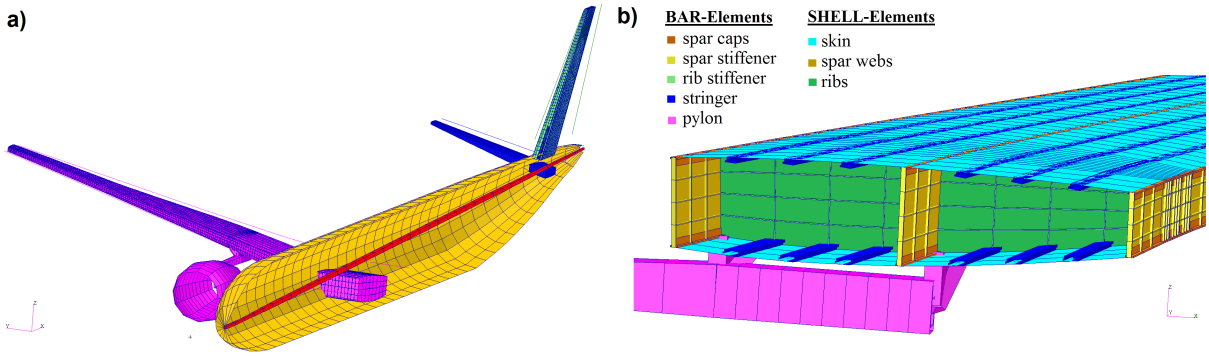

Figure 4: a) half of the full structural finite element model of the complete aircraft configuration, b) structural modelling details of the wing box and the pylon.

In order to reduce the computational time for the 1062 load cases considered during the loads process, the stiffness from the full GFEM/Dynamic is condensed to reduce the considered degrees of freedom. Not only the stiffness but also the mass matrix must be condensed to the LRA points to reduce the computational effort. The single masses and their moments of inertia are concentrated to the nearest LRA-point (see Figure 5a). The full GFEM/dynamic consists of about 18.000 FE-nodes and roughly 42.000 FE-elements. The condensed GFEM/dynamic model consists solely of 471 FE-nodes and 134 FE-elements (RBE2) like shown in Figure 5c). Another needed model for loads analysis is the aerodynamic model. Figure 5b) shows the mesh for the VLM/DLM analysis within MSC Nastran. For further information about the aerodynamic model see [23].

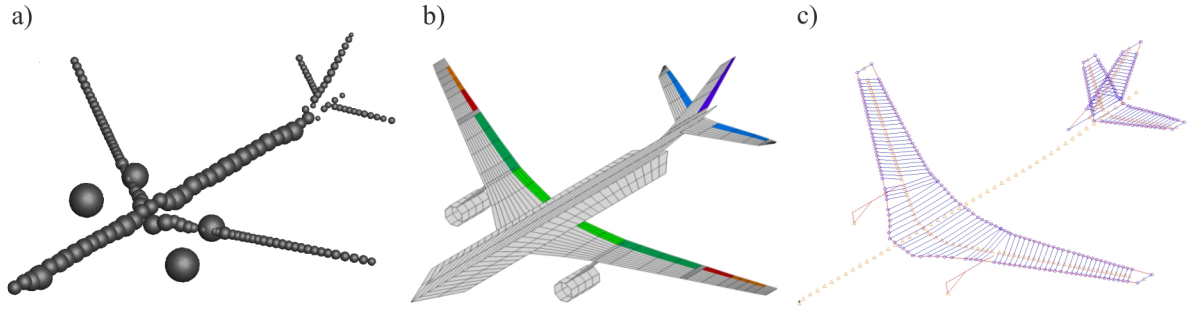

Figure 5: MSC Nastran simulation models, a) mass model, b) aerodynamic model, and condensed structural model.

5 APPLICATION OF CPACS-MONA

In the first part of this paragraph, the stand-alone application of cpacs-MONA will be shown for the prior mentioned reference configuration. In the second part, a parameter study of the XRF1-DLR is shown, where the aspect ratio and the sweep angle of the leading edge will be varied. This parameter variation has been generated using a CAD-ROM creating new Tecplot profile cuts of the outer geometry. The optimized GFEM/Dynamic of these parameter variations, as output of cpacs-MONA, are afterwards used for an aerodynamic flight performance analysis using CFD to get a superior evaluation of the configurations. In the last part of this paragraph, the integration of cpacs-MONA in a gradient-free high fidelity MDO environment will be investigated.

5.1 Aeroelastic structural design of the reference configuration

The aeroelastic design process is run through for the XRF1-DLR baseline configuration and rerun until convergence with respect to the structural wing mass and the loads is achieved. Regarding the amount of time needed for the various phases of cpacs-MONA the following has been determined: cpacs-MONA consumes about ten minutes to set up all the simulations and optimization models together with conceptual design loads estimation and preliminary sizing. About fifteen minutes elapses for the loads calculation and the selection of the design load cases. Another six minutes are needed for the structural optimization of the main wing, the horizontal and the vertical tailplane. For the main wing a second structural optimization takes places with the aileron efficiency as constraint. A complete cpacs-MONA run takes in average three iterations for the convergence for the mass and loads. In total it takes almost two hours for the complete aeroelastic structural design of an aircraft configuration as detailed and large as the XRF1-DLR.

For this paper, cpacs-MONA is considers six different mass cases for the loads analysis. The mass cases are a combination of the operating empty weight (OWE) together with defined payload/passenger variations and the fuel conditions. The passengers will be distributed within the fuselage cabin according to the defined seats and the fuel is located in the fuel tanks located within the wing box (center, inner and outer tank) and a trim tank within the horizontal tailplane. Table 2 gives an overview of the considered mass cases and the composition of fuel and payload/passenger conditions.

Table 2: Overview of the mass cases – a combination of payload and fuel.

	MOOee	MTOAa	MTOfF	MZOAe	MFOeF	MCRUI
Design Mass	OWE	MTOW	MTOW	MZFM	-	Cruise
Payload	0%	100%	20%	100%	0%	100%
Fuel	0%	64%	100%	0%	100%	25 %

Figure 6 shows the resulting mass and center of gravity (CG) diagram of the XRF1-DLR reference configuration together with the borders for stability and control in percentage of the mean aerodynamic chord (MAC).

For the current version of cpacs-MONA the mass model is not required to achieve a fixed target center of gravity (e.g. most forward or most rearward positions). The available mass items are taken from the CPACS dataset and distributed reasonably for each component. To achieve the extreme loads and to guarantee a better comparability in case of parameter studies as done in section 5.2, it is planned to set target center of gravity positions for the mass cases, e.g. fixed percentages of mean aerodynamic chord. As can be seen in Figure 6, the center of gravity range for the reference configuration covers about 50% of the area from most forward at 10% MAC and most rearward at 40% MAC.

For each mass case various different load types are calculated. These include pull-up, push-down, yawing, rolling and quasi-stationary gust encounters for different flight levels and design speeds according to CS25.335. In total 1062 load cases are considered within the loads analysis part of cpacs-MONA.

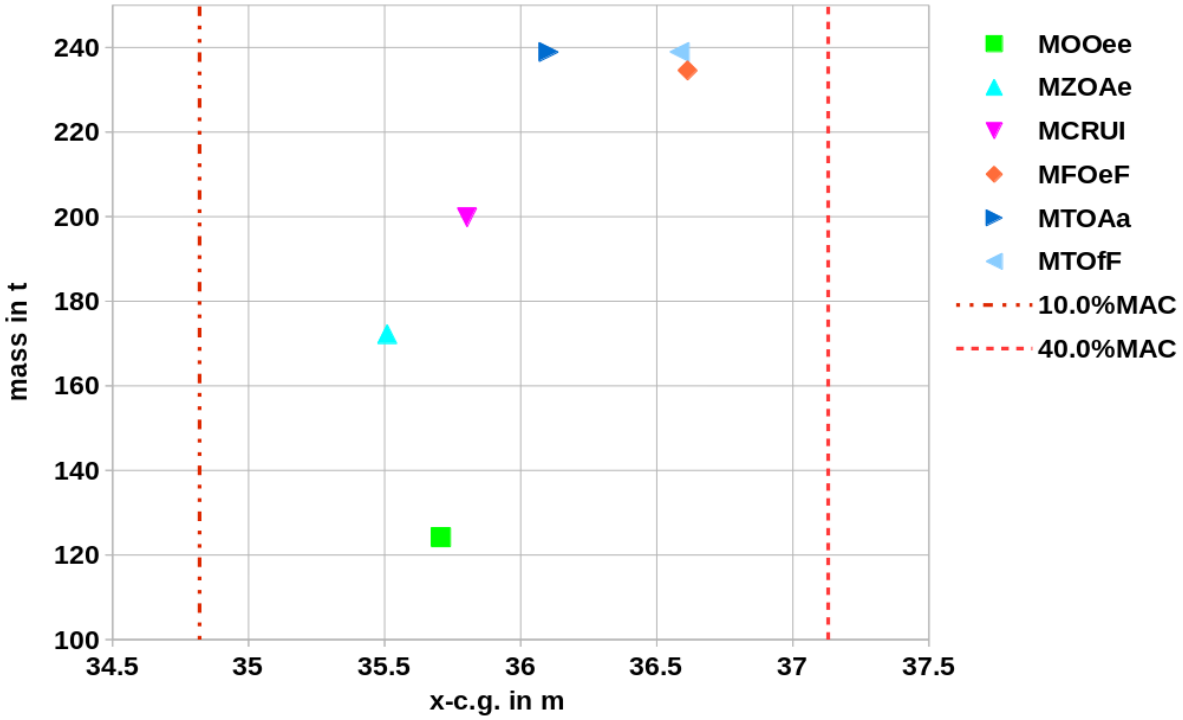

Figure 6: Mass-CG-diagram of the XRF1-DLR reference configuration.

In cpacs-MONA, there are two different ways to evaluate the design loads. On the on hand, there is the 1-D approach, where the maximum SMT-loads per component and per load reference axis point with a corresponding coordinate system are identified. The 1-D method is used for the preliminary sizing of the structure. For the estimation of the design loads for the structural optimization in addition to the 1-D approach, a 2-D evaluation is available. Therein, for the combination of two selected cutting load components for each load reference axis point, the load cases on the convex hull are defined as design loads. The combined cutting load components are F_z/M_x and M_x/M_y. Figure 7 shows such a 2-D cutting loads envelope for the main wing at the LRA-point located at y=8.8m. The 2-D approach leads to a higher number of load cases.

The maximum bending moment in Figure 7 is caused by a pull-up maneuver for the maximum take-off weight configuration with the forward located center of gravity position. The same mass case causes the minimum bending moment at a push-down maneuver and the maximum and minimum torsion moment likewise with the same maneuvers. The maximum loads mostly occur at a high altitude and the design speeds V_C and V_D.

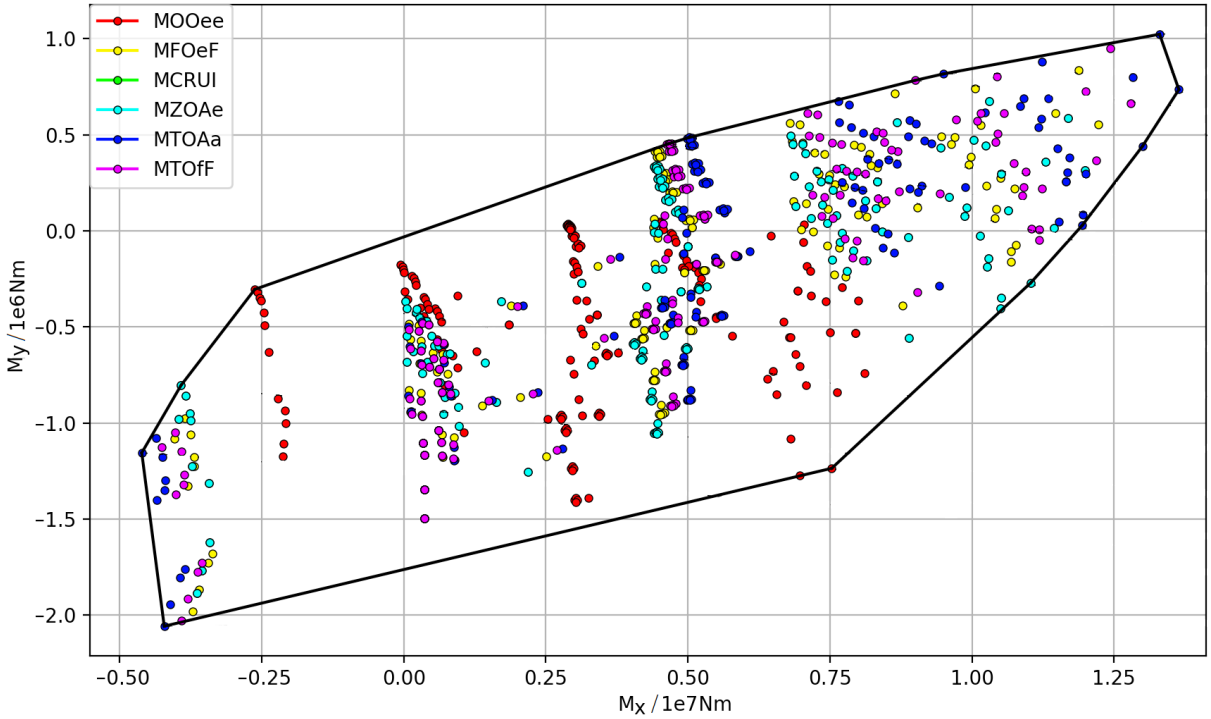

Figure 7: Loads envelope for M_x vs. M_y for the wing @ y=8.8m.

The structural optimization of the main wing together with the control surface efficiency optimization leads to a converged total mass of the main wing of 37305 kg. Compared to the DLR's conceptual aircraft design tool VAMPZero [24] the wing mass estimated with cpacs-MONA is about 8.7% (34325 kg) larger. Though, a comparison to another conceptual weight estimation method for wings, developed at DLR-AE [25], the wing from cpacs-MONA is only 5.8% (35260 kg) heavier. Therein, also the loads of the flexible structure are taken into account.

The thickness distribution of the wing can be seen in Figure 8. Figure 8a) shows the thickness of the upper skin and the front spar, where Figure 8b) displays the thickness of the lower skin and the rear spar. The increase of the upper skin thickness at the rear part in the first third of the wing span (yellow design field) is a result of the considered landing loads. The gross

thickness distribution can be seen at the lower skin in the front part after the engine position. The decreasing skin thickness around the attached pylon can be explained by additional element out of titian at the upper and lower skin and at the rear and front spar that are not displayed. Such elements are used as additional reinforcement structure. The reason of this provision is that the structural optimization without the reinforcing elements led to an excessive and unrealistic increase of the thickness variables in this area.

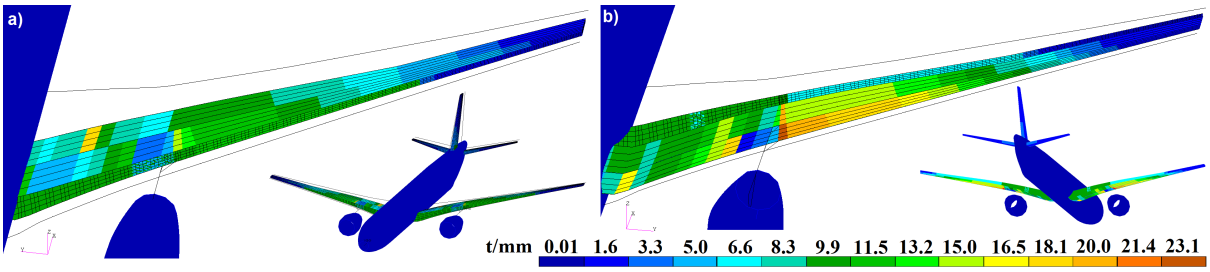

Figure 8: Thickness distribution of the main wing - XRF1-DLR baseline – a) upper-front-view; b) lower-rear-view.

5.2 Parameter study of the reference configuration

For this parameter study, the aspect ratio and the sweep angle of the leading edge of the XRF1-DLR configurations wing was varied. The two parameters will be varied individually and combined. This leads to nine different configurations. The planform of these nine configurations are shown in Figure 9. The reference configuration will further be called BASELINE. “AR+1” means, that the aspect ratio increases about five percent and “SW-1” means, that the sweep angle decreases about one degree. “AR-1_SW+1” leads to the configuration, where the aspect ratio decreases about 5 percent and the sweep angle increases simultaneously about one degree and “AR+1_SW-1” is the vice versa case.

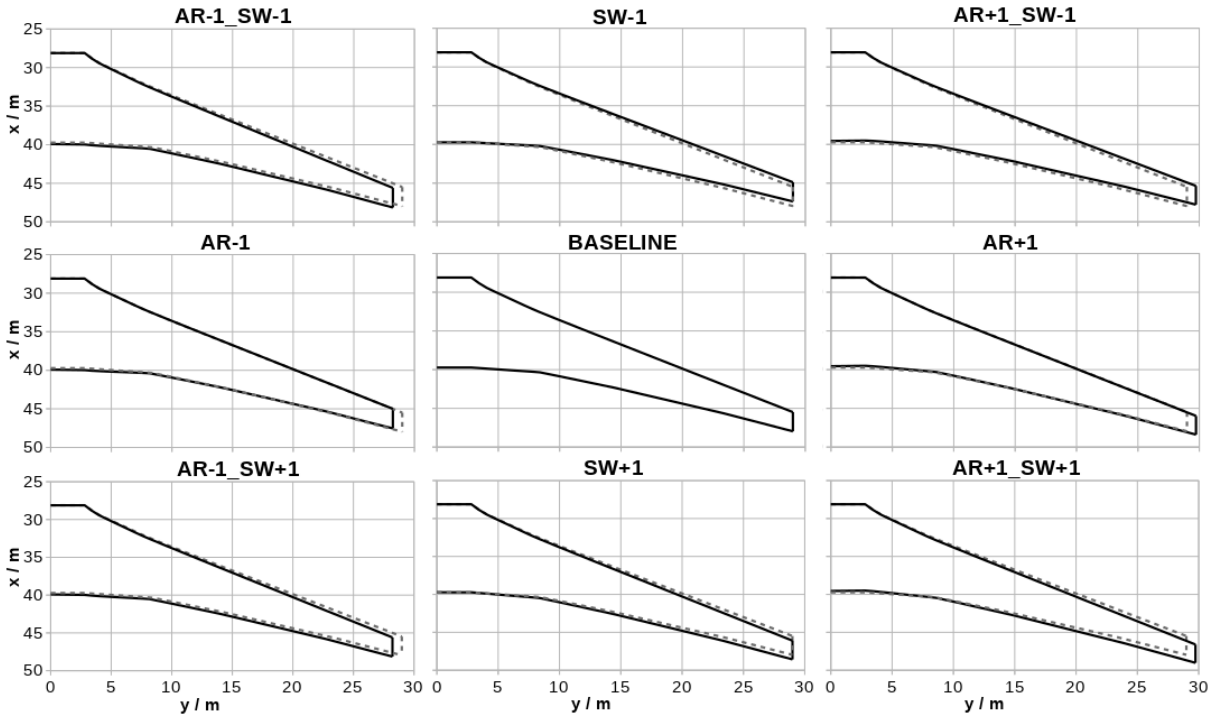

Figure 9: Planform variations of main wing.

The main results of the performed parameter study are listed in Table 3. Therein the percentage variances with respect to the BASELINE values are presented. First of all the effect of the variations on the mass and the wing tip displacement are investigated. The tip displacement in *z*-direction reflects the wing stiffness. A decrease of the tip displacement means that the stiffness of the wing in bending direction increases. Next, the effect on the wing bending moment (M_x) and the wing torsional moment (M_y) is explained, followed by the presentation of results from aero-structure coupled CFD analysis.

Table 3: Results of the parameter variation.

Variation	Wing mass, kg	Max M_x, Nm	Max M_y, Nm	Contr. Surf. Eff.	Max z disp, m	C_D	AoA, deg
SW-1	-0.86 %	-0.82 %	-0.66 %	1.33 %	-2.08 %	1.34 %	-3.24 %
AR-1_SW-1	-5.72 %	-3.60 %	-0.28 %	1.79 %	-9.89 %	0.86 %	-7.28 %
AR-1_SW+1	-3.99 %	-1.89 %	0.92 %	-1.29 %	-5.10 %	-0.62 %	0.55 %
AR-1	-4.19 %	-2.65 %	0.33 %	0.34 %	-7.57 %	-0.10 %	-3.76 %
BASELINE	100%	100%	100%	100%	100%	100%	100%
AR+1	3.57 %	1.30 %	-3.22 %	-2.21 %	8.42 %	0.21 %	4.38 %
AR+1_SW-1	2.25 %	0.48 %	-3.71 %	-3.31 %	6.15 %	1.43 %	0.83 %
AR+1_SW+1	3.95 %	-1.76 %	1.41 %	-6.21 %	11.07 %	-0.46 %	8.33 %
SW+1	0.02 %	0.59 %	0.53 %	-5.65 %	2.76 %	-0.54 %	4.39 %

For all variants above the BASELINE in Table 3 the resulting wing mass values and the maximum tip displacements are diminished. Furthermore configuration with combined variation of wing sweep and aspect ratio exhibit to some extent a superposition characteristic. For the AR-1 and the SW-1 variations separately the wing mass and the tip displacement are reduced. The AR-1_SW-1 configuration, where both parameters are varied simultaneously, exhibits an even higher reduction of the wing mass and the wing tip deflection as for the separate variants. For the AR-1_SW+1 configuration though, the increased wing sweep angle leads to a more slight decrease in the wing mass as compared to the AR-1 configuration. That can be explained by the fact that the increase of the sweep angle counteracts not fully the effects of lower wing mass and higher wing stiffness due to the decreased wing aspect ratio. The opposite trend can be observed for the variations listed below the BASELINE configuration.

Even for the control surface efficiency the superposition characteristic for combined aspect ratio and wing sweep variation can be identified. For separate and combined higher aspect ratio and higher sweep angle control surface efficiency is reduced. The configuration AR+1_SW-1 is still under investigation as the control surface efficiency is worse than AR+1 alone. Though for AR+1_SW-1 the reduced wing sweep is expected to have a counteracting effect on the control surface efficiency.

Altogether the understanding of the results of the combined variations is still vague, especially regarding the assumption of a superposition characteristic. It is therefore worth to furthermore scrutinize all analysis data of the corresponding variants (e.g. loads data, structural optimization results.

Regarding the separate variation of the aspect ratio and the wing sweep the investigation of the wing loads is presented next. In Figure 10 the convex hull for the bending (M_x) and torsion (M_y) moment of the main wing at a y-position of 8.8 meters is displayed. Figure 10a) shows the effect of the sweep angle on the convex hull of the cutting moments. The influence on the maximum and minimum cutting moment is with less than one percent rather small. But it can be seen, that the increase of the sweep angle narrows the convex hull at the negative cutting moments. And a more forward swept wing leads to a widening of the envelope. The small mass change due to the change in the wings sweep can also be correlated to the small change in maximum and minimum cutting moments.

In Figure 10b) the effect of the aspect ratio is shown. It can be seen, that the variation of the aspect ratio leads to a rotation of the convex hull. An increase of the aspect ratio results in a clockwise rotation with higher maximum bending moment M_x and lower maximum torsional moment M_y. The decrease of the aspect ratio exhibits a counter-clockwise rotation of the envelope with lower maximum wing bending moment M_x and higher maximum torsional moment M_y.

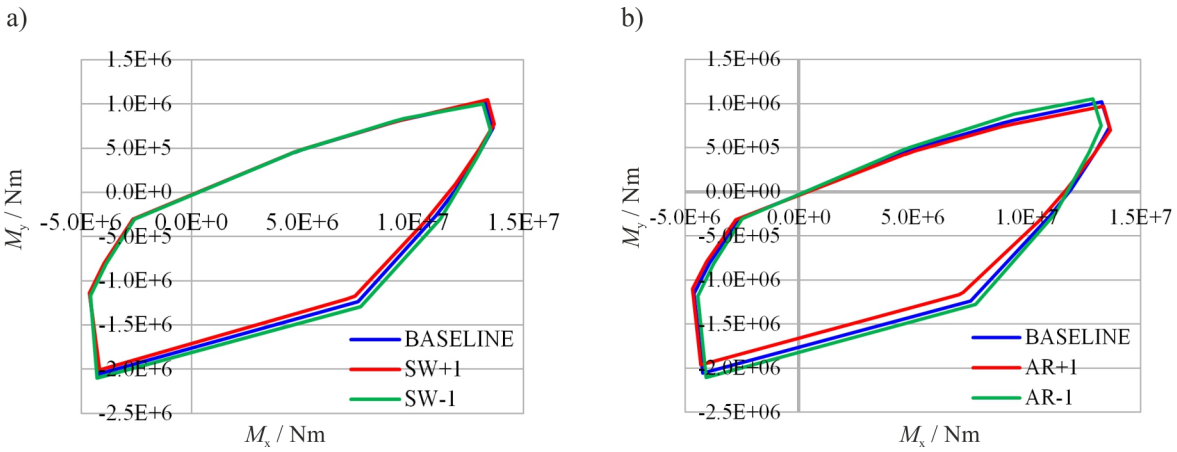

Figure 10: 2-D cutting loads M_x vs. M_y at the wing root for a) wing sweep and b) aspect ratio variation.

After the completion of cpacs-MONA a CFD-CSM analysis is done to check the performance characteristics and estimate the aerodynamic drag C_D for cruise condition (Ma 0.83, altitude 11000m). Exemplarily CFD results for the aspect ratio variations AR+1 and AR-1 are displayed in Figure 11. It can be seen, that the higher mass of the AR+1 configuration leads to a higher angle of attack and correspondingly to a higher drag. Another aspect, why the drag of the AR+1 configuration is even worse compared to the BASELINE, is the fact that the airfoils are not optimized for AR+1. It should be furthermore mentioned that the AR+1 configuration exhibits a more forward located position of the center of gravity in terms of percentage of the mean aerodynamic chord (MAC). This is also the reason why the horizontal tailplane had to produce more downwash, which in addition increased the trim drag.

The coupled aero-structural CFD analysis results underscore also the necessity to adapt the trim conditions, the mass configuration, or the center of gravity position, with the objective to achieve comparable trim analysis for the cruise condition.

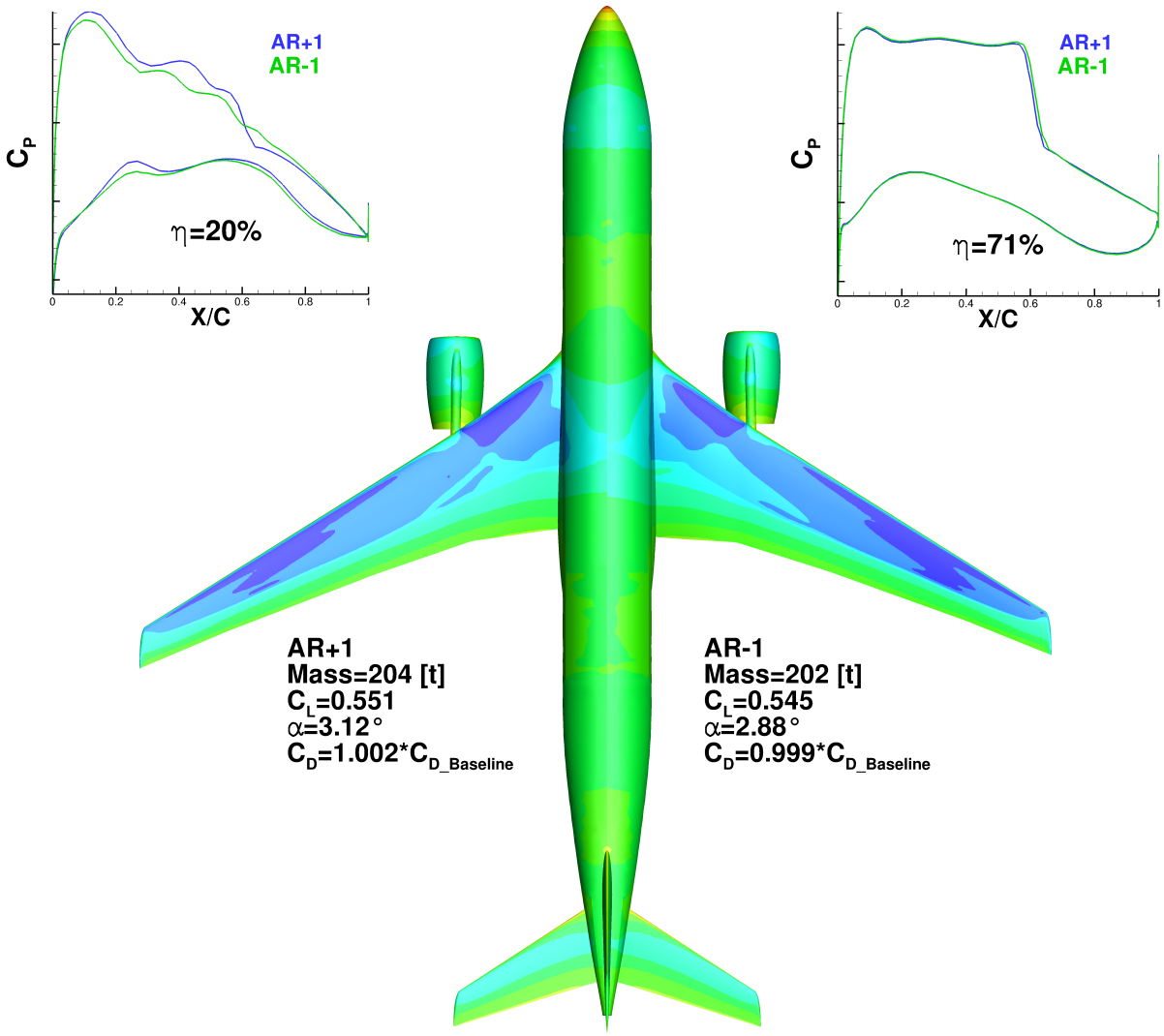

Figure 11: Comparison of the CFD results for the AR+1 and AR-1 configurations.

5.3 Application of cpacs-MONA in a gradient-free high-fi based MDO environment

On the one hand cpacs-MONA can be used as a stand-alone tool, as shown in section 5.1 and 5.2. Within the DLR project VicToria cpacs-MONA was also used as one tool within a high-fidelity based MDO approach called cybermatrix protocol. The cybermatrix protocol is an MDO concept, where on the one hand high performance computing is about to be used to full capacity and on the other hand the couplings of the involved disciplines are provided as approximate cross-disciplinary scaled sensitivities, called “approximate Jacobiens”. This concept is with regards to typical aircraft design processes respectively MDO implementations seen as a compromise between a classical aircraft design processes with as many disciplines as possible, stringed sequentially, and more or less loosely coupled, and MDO approaches with tight coupling of a rather small number of disciplines. The latter normally employ formal mathematical optimization techniques.

For an aero-structural coupled system, a structural design process could provide the aerodynamic design process with the elastic deflection of the wing at the flight point or the change of the wing mass with respect to the airfoil thickness. The latter would be a design coupling. The disciplinary design processes run more or less independent, the coupling happens through defined data exchanges between the disciplines. As disciplinary design

process can have different expenditure of time, the frequency of data exchange between the disciplinary design processes can be different. Further details of a cybermatrix protocol developed by DLR-AS are outlined in [6]. It is not intended to discuss the concept herein in great detail. The focus in this paper is rather to take the application of [6] and discuss the results regarding the structural design. That part was taken over by cpacs-MONA.

In Figure 12a) the cybermatrix representation of the application for the XRF1-DLR is shown. Three disciplines are involved: aerodynamic design of airfoil shapes (aero), structural optimization of the wing (struct), and determination and evaluation of design loads for the structural optimization (loads).

The *aerodynamic design of airfoil shapes* is done with the FlowSimulator environment. It uses an adjoint-gradient based aerodynamic optimization method. The objective is drag minimization, with aeroelastic coupling for the trim analysis. The CFD mesh is hybrid unstructured and contains 544 000 point and 1 130 000 elements. As reference cruise flight point Mach 0.83 and an altitude of 11000 m are taken.

The *structural optimization of the wing structure* is performed by cpacs-MONA. Details of cpacs-MONA and the XRF1-DLR structural model are already mentioned in the paper. The objective herein is the minimization of the wing mass. During the optimization, updated airfoil shapes are obtained from the aerodynamic sub process and updated external design loads from the loads sub process.

Determination and evaluation of design loads is performed by VarLoads framework [26] plus the loads calculated within cpacs-MONA. Beyond the quasi-static loads from cpacs-MONA VarLoads also performs transient dynamic simulations of gust and turbulence excitation as well as selected closed loop maneuvers using flight control laws. The structural and aerodynamic model is provided by cpacs-MONA.

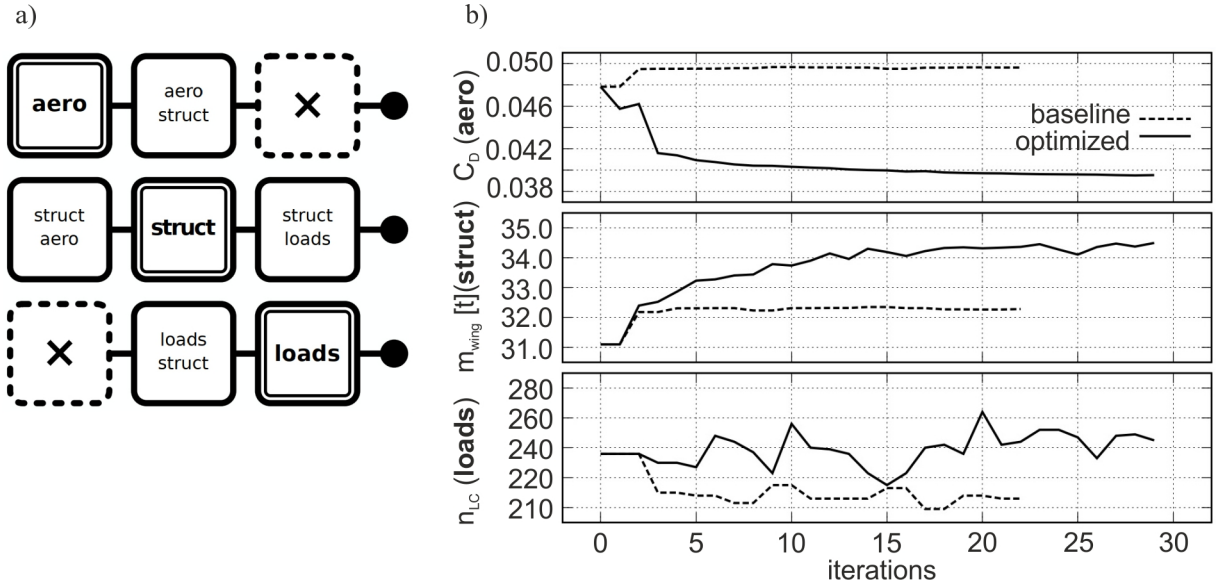

Figure 12: a) Cybermatrix representation of the application, b) convergence history of the overall MDO process, total run time 110 hours on 64 cores.

The convergence of the cybermatrix protocol MDO process is displayed in Figure 12b). Three quantities of interest, one for each sub process are shown. The drag coefficient for the whole configuration C_D, the mass of the wing m_{wing}, and the number of the selected design load cases n_{LC}.

The changing number of the design load cases reflects the characteristic of the 2-D approach for the selection of the design loads mentioned in section 5.1. The number of load cases on the described convex hull can vary over the loads analysis iterations. For the baseline configuration the number of load cases varies, though the aerodynamic design doesn't change. This effect shows that even for the almost same wing weight the structural design changes in a way that the loads analysis leads to a varying number of load cases.

The history of the wing mass m_{wing} shows an increase of about 2t compared to the converged baseline value at iteration 5. This shows the known trade-off between the objectives to minimize drag and to minimize the structural mass. With a further calibration of the cybermatrix protocol MDO process, the relation of aerodynamic and the structural objective can be adjusted. Compared to the results shown in section 5.1, the wing mass is about 5t lower. This can be explained by the fact that for the cpacs-MONA here the landing loads were not yet included.

An interesting aspect regarding the interdependence of aerodynamic design, loads analysis, and structural optimization can be observed in Figure 13. In a, the variation of the wing twist from iteration 0 (baseline) to iteration 6 is shown. The minimal variation of the wing twist resulted in a somewhat complex variation of the structural design. On the one hand the twist of iteration 6 leads to a heavier structural weight. This can be retraced by the domination of a thickness increase shown in Figure 13b). Though, parts of the structure experience a decrease of thickness for the outer wing and the front center wing box. This result underlines the necessity to scrutinize optimization results on disciplinary level. A conclusion in this case would be that besides of the fact that iteration 6 has a higher wing weight, nevertheless some minor benefits of iteration 6 can be observed and should not be neglected.

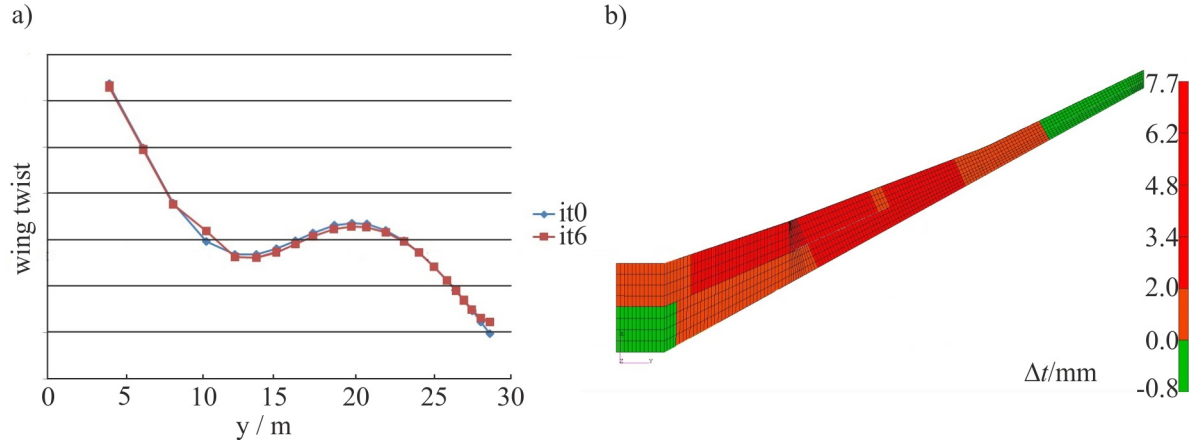

Figure 13: a) Wing twist of the initial (it0) and final aerodynamic design (it6), b) difference of skin thickness for initial and final structural design.

6 CONCLUSION

In the paper the aeroelastic structural design process cpacs-MONA developed at DLR-AE is presented. The basic parametrization concept and the core elements: parametric model set-up, loads analysis, and structural optimization, coming from MONA, are shown as well as the far-reaching completion of the design process, the interfacing with CPACS, and its automatization to the point of an applicable tool in DLR-wide MDO environments.

The application of cpacs-MONA to the XRF1-DLR shows reasonable results compared to conceptual design methods. The parameter study with variations of the wing sweep and the wing aspect ratio delivered plausible results. The comparison with conceptual design tools revealed reasonable differences and underscored the necessity to incorporate analysis methods from preliminary design in early design stages where still the wing planform is not frozen.

The utilization of cpacs-MONA in a new high-fidelity based MDO concept, the cybermatrix protocol, shows the smooth interfacing of cpacs-MONA with high-fidelity aerodynamic or coupled aero-structural analysis. The view in the paper on the results of the structural optimization of the briefly described application shows also a potential due to a differentiated evaluation of the optimization result.

Especially the field of high-fidelity aero-structural analysis offers further opportunities for the further development of cpacs-MONA. Herein the inclusion of CFD or CFD/CSM results to improve the VLM/DLM aerodynamic analysis of cpacs-MONA is promising. Regarding the loads analysis, further types of loads e.g. gust loads, continuous turbulence, and maneuver and gust loads with flight control system should be included as well.

Regarding the material, the inclusion of composite material in the automatized process is a next step as well as the final incorporation of the already available detailed structural model for the fuselage.

7 REFERENCES

[1] MSC Software. *MSC.Nastran 2004 Design Sensitivity and Optimization User's Guide*, 2003.

[2] N.N. *ASTROS - User's Reference Manual for Version 20*. Universal Atlantics, Inc., 1997.

[3] R. Zotemantel. MBB-LAGRANGE: A Computer Aided Structural Design System. In H.R.E.M. Hörnlein and K. Schittkowski, editors, *Software Systems for Structural Optimization*, volume 110 of *International Series of Numerical Mathematics*, pages 143–158, Basel, Boston, Berlin, May 1998. Birkhäuser Verlag. ISBN: 3-764-32836-3.

[4] J. Dillinger, T. Klimmek, M. M. Abdally, and Z. Gürdal. Stiffness Optimization of Composite Wings with Aeroelastic Constraints. *Journal of Aircraft*, 50(4):1159–1168, July 2013.

[5] G. K. W. Kenway, G. J. Kennedy, and J. R. R. A. Martins. Aerostructural optimization of the common research model configuration. In *15th AIAA/ISSMO Multidisciplinary Analysis and Optimization Conference, 16-20 June, 2014, Atlanta (GA, USA)*, Atlanta, GA, June 2014.

[6] C. Ilic, A. Merle, A. Ronzheimer, M. Abu-Zurayk, J. Jepsen, M. Leitner, M. Schulze, A. Schuster, M. Petsch, and S. Gottfried. Cybermatrix: A novel approach to computationally

and collaboration intensive MDO for transport aircraft design. In *STAB2018, 21. DGLR-Fach-Symposium der STAB, 6.-7. November 2018, Darmstadt*, 2018.
[7] S. Görtz, Ilic C., Jepsen J., Leitner M., Schulze M., Schuster A., Scherer J., Becker R.-G., Zur S., and Petsch M. Multi-Level MDO of a Long-Range Transport Aircraft Using a Distributed Analysis Framework. In *AIAA-2017-4326. 18th AIAA/ISSMO Multidisciplinary Analysis and Optimization Conference, 5.-9. Jun. 2017, Denver, USA.*, 2017.
[8] S. Keye, T. Klimmek, M. Abu-Zurayk, M. Schulze, and C. Ilic. Aero-Structural Optimization of the NASA Common Research Model. In *18th AIAA/ISSMO Multidisciplinary Analysis and Optimization Conference, AIAA Aviation and Aeronautics Forum and Exposition, Denver, Colorado, 5-9 June 2017*, 2017.
[9] T. Klimmek. *Statische aeroelastische Anforderungen beim multidisziplinären Strukturentwurf von Transportflugzeugflügeln*. Dissertation, TU-Braunschweig, August 2016. DLR-FB 2016-34.
[10] T. Klimmek. Parametric Set-Up of a Structural Model for FERMAT Configuration for Aeroelastic and Loads Analysis. *Journal of Aeroelasticity and Structural Dynamics (ASD Journal)*, 3(2):31–40, 2014.
[11] A. Voss and T. Klimmek. Design and Sizing on a Parametric Structural Model for a UCAV Configuration for Loads and Aeroelastic Analysis. *CEAS Aeronautical Journal*, 8:67–77, March 2017.
[12] K. Bramsiepe, V. Handojo, M. Y. Meddaikar, M. Schulze, and T. Klimmek. Loads and Structural Optimization Process for Composite Long Range Transport Aircraft Configuration. In *AIAA AVIATION Forum 2018, Multidisciplinary Analysis and Optimization Conference, 25-29 June 2018, Atlanta (GA, USA)*, 2018.
[13] W. R. Krüger and S. Cumnuantip. A Hybrid Approach for the Analysis of Aircraft Ground Loads. In *IFASD2019, International Forum on Aeroelasticity and Structural Dynamics, 10-13 June 2019, Savannah, GA (USA)*, 2019.
[14] R. Liepelt, V. Handojo, and T. Klimmek. Aeroelastic analysis modelling process to predict the critical loads in an MDO environment. In *IFASD International Forum on Aeroelasticity and Structural Dynamics, 28 June - 2 July, 2015, Saint Petersburg (Russia)*, 2015.
[15] B. Nagel, D. Böhnke, V. Gollnick, P. Schmollgruber, A. Rizzi, and G. La Rocca J.J. Alonso. Communication in aircraft design: Can we establish a common language? In *ICAS, 28th International Congress of the Aeronautical Sciences, 23-28 September 2012, Brisbane (Australia)*, 2012.
[16] J. Fuchte. *Enhancement of Aircraft Cabin Design Guidelines with Special Consideration of Aircraft Turnaround and Short Range Operations*. Dissertation, 2014.
[17] N.N. The USAF Stability and Control DATCOM, Volume 1. Users Manual AFFDL-TR-79-3032, McDonnell Douglas Astronautics Company, April 1979. Updated by Public Domain Aeronautical Software, December 1999.
[18] D. J. Farrar. The Design of Compression Structures for Minimum Weight. *Journal of the Royal Aeronautical Society*, 53:1041–1052, November 1949.
[19] J. Pattinson and M. Herring. High Fidelity Simulation of Wing Loads with an Active Winglet Control Surface. In *IFASD 2013, International Forum on Aeroelasticity and Structrual Dynamics, 24-26 June 2013, Bristol (GB)*, 2013.
[20] M. Siggl, J. Kleinert, T. Stollenwerk, and R. Maierl. TiGL An Open Source Computational Geometry Library for Parametric Aircraft Design. *Mathematics in Computer Science. Springer. ISSN 1661-8270 (eingereichter Beitrag)*.
[21] N. Kroll, M. Abu-Zurayk, D. Dimitrov, T. Franz, T. Führer, T. Gerhold, S. Görtz, R. Heinrich, C. Ilic, J. Jepsen, J. Jägersküpper, M. Kruse, A. Krumbein, S. Langer, D. Liu, R. Liepelt, L. Reimer, M. Ritter, A. Schwöppe, J. Scherer, F. Spiering, R. Thormann, V. Togiti,

and D. Vollmer J.-H. Wendisch. DLR Project Digital-X: towards virtual aircraft design and flight testing based on high-fidelity methods. *CEAS Aeronautical Journal*, 7, 2016.
[22] S. Görtz, A. Krumbein, M. Ritter, and J. Hofmann. DLR-Projekt VicToria - Virtual Aircraft Technology Integration Platform. In *DLRK2018, Deutscher Luft- und Raumfahrtkongress, 4-6 September 2018, Friedrichshafen (Germany)*, 2018.
[23] M. Leitner, R. Liepelt, T. Kier, T. Klimmek, and R. Müller M. Schulze. A Fully Automatic Structural Optimization Framework to Determine Critical Loads. In *DLRK2016, Deutscher Luft- und Raumfahrt Kongress, 12-15 September 2016, Braunschweig (Germany)*, 2016.
[24] D. Böhnke, B. Nagel, and V. Gollnick. An Approach to Multi-Fidelity in a Distributed Design Environment. In *IEEE Aerospace Conference, Big Sky, USA, 2011*, 2011.
[25] G. Chiozzotto. Wing weight estimation in conceptual design: a method for strut-braced wings considering static aeroelastic effects. *CEAS Aeronautical Journal*, 7(3):499–519, 2016.
[26] T. M. Kier and G. H. N. Looye. Unifying Manoeuvre and Gust Loads Analysis Models. In *IFASD, International Forum on Aeroelasticity and Structural Dynamics, 21-25 June 2009, Seattle, WA (USA)*, 2009.

COPYRIGHT STATEMENT